

Development of an automated pump efficiency measuring system for ozonesondes utilizing ~~an~~the airbag-type flowmeter

Tatsumi Nakano^{1, a}, Takashi Morofuji²

¹Aerological Observatory, Japan Meteorological Agency, 1-2, Nagamine, Tsukuba-shi, Ibaraki 305-0052, Japan

²Atmosphere and Ocean Department, Japan Meteorological Agency, 3-6-9, Toranomon, Minato-~~ku~~city, Tokyo 105-8431, Japan

^aCurrently at: Fukuoka Regional Headquarters, Japan Meteorological Agency, 1-2-36, Ohori, Chuo-ku, Fukuoka-shi, Fukuoka 810-0052, Japan

Correspondence to: Takashi Morofuji (morofujitakashi@met.kishou.go.jp)

Abstract. ~~We here report on~~~~We have developed~~ a system ~~developed~~ to automatically measure the flow rate characteristics (i.e., the pump efficiency) of the pumps ~~onbuilt in the~~ ozonesondes, so-called “pump efficiency”, under various pressure levels/situations ~~simulating/emulating~~ upper-air conditions. The system consists of a flow measurement unit ~~incorporating that~~ uses a polyethylene airbag, a pressure control unit that reproduces ~~a~~ low-pressure environmental conditions, and a control unit that integrates and controls these ~~elements to, and~~ enables fully automatic measurement. The Japan Meteorological Agency (JMA) ~~has been~~ operationally measuring the pump efficiency ~~for of the~~ Electrochemical Concentration Cell (ECC) ozonesondes using the system since 2009, ~~resulting in a significant body of related and has collected/accumulated~~ a lot of measurement data. ~~Extensive measuring data collected for~~ ~~From the multiple measurements of~~ the same ozonesonde pump ~~over a period of for~~ around 12/twelve years ~~indicate, we confirmed~~ the long-term stability of the system’s performance. ~~The se~~ long-term ~~measurement~~ data also showed that ~~ozonesonde/the~~ pump flow characteristics ~~of ozonesondes~~ differed among production lots. ~~We evaluationed of~~ the impacts of ~~the~~ variance in these characteristics on ~~the~~ observed ozone concentration data, ~~as compar~~ed with ~~to the~~ reference ozone profiles, ~~indicated and found~~ that the influences on total ozone estimation was ~~up to approx. about~~ 4% ~~to the maximum~~, the standard deviation per lot was ~~approx. about~~ 1%, and the standard deviation among lots was ~~approx. about~~ 0.6%.

1 Introduction

Atmospheric ~~o~~Ozone ~~in the atmosphere~~ protects the biosphere by absorbing harmful ultraviolet radiation. ~~In order to monitor the destruction of the ozone layer due to the release of chemical substances caused by human activities. In this context,~~ the World Meteorological Organization (WMO) ~~plays a~~has taken the leading role in observing ozone profiles on a global scale ~~to monitor ozone layer deterioration caused by chemical release from human activity~~ (Smit et al., 2021).

Ozonesonde observations are the only means of directly ~~determining the actual/obtaining~~ ~~the detailed~~ vertical distribution of ozone from the troposphere to the lower stratosphere. The ozonesonde ~~model used for such observations~~ is a balloon-borne

コメントの追加【諸藤1】: Proofreading by a native speaker.

The following corrections without comments are due to the Proofreading by a native speaker.

コメントの追加【諸藤2】: Replaced according to Referee#1

コメントの追加【諸藤3】: Replaced according to Referee#1

コメントの追加【諸藤4】: Replaced according to Referee#1

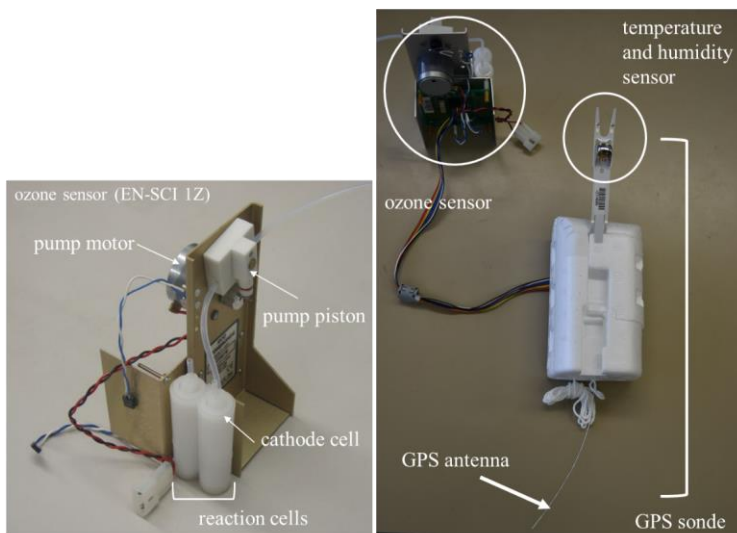


Figure 1: Appearance of the ozone sensor of the ECC-type ozonesonde ozone sensor (left) and connected GPS sonde connected to the ozone sensor (right).

Figure 2 ~~illustrates~~ shows how the pump operations. Firstly, ~~the~~ ambient air taken into the pump is compressed until its pressure is balanced with the back-pressure ~~associated with~~ due to the hydraulic head pressure of the reaction cell ~~and a Teflon rod in the reaction cell~~ (1). The compressed air is then discharged to the cell by the force of the piston (2). When the piston is completely pushed in, there is a dead space inside the pump (3), and the compressed air remaining in it expands until it is balanced with the ambient air pressure (4). ~~The piston draws in a fresh sample of ambient air~~ Then again, the force of the piston takes the ambient air into the pump (5). ~~The cycle is repeated for each pump rotation. The steady pump speeds typically range from 2,400 – 2,600 rotations per minute (RPM). During the ozonesonde observation, this cycle is repeated.~~ Hydraulic head pressure, which is the main factor causing back-pressure, can be considered essentially uniform regardless of ambient air pressure. The back-pressure could be assumed nearly identical at the ground-level pressures and at lower pressures in the upper air, while the latter varies but the ambient air pressure is different along with the altitude. Under these conditions, the air taken in is more compressed in step (1) and the air in the dead space is more expanded in step (4). In other words, as the ambient air pressure decreases, the intake-air volume of air intake (=pump flow rate) into the reaction cell also falls. Thus, as a consequence, the pump is affected by the ambient air pressure, which governs its called the pump efficiency.

コメントの追加【諸藤13】: Since the influence of the Teflon rod is not important here in explaining the concept that pump efficiency arises, so we removed.

コメントの追加【諸藤14】: Replaced according to Referee#2

コメントの追加【諸藤15】: Replaced according to Referee#2

コメントの追加【諸藤16】: Replaced references according to Referee#2's comment
 "Lines 47-48: I am having difficulty in understanding the first part of this sentence. I believe this is saying the back pressure is always the same from ground level to low pressure while ambient pressure is decreasing."

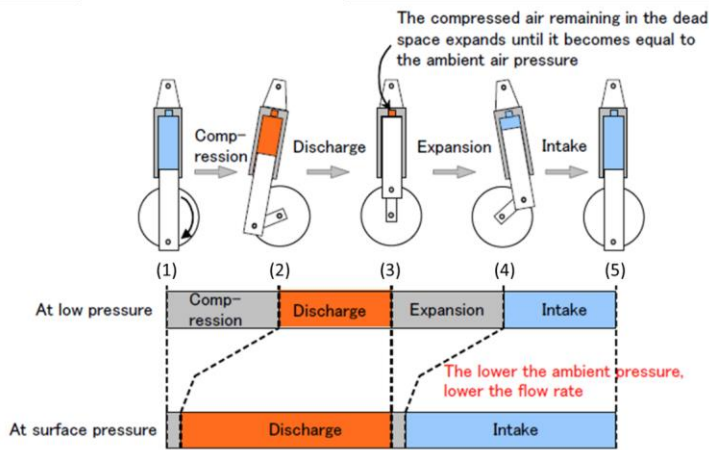


Figure 2: ~~Explanation of how the piston pump operations during observation, and effect of how the dead space on of the pump affects pump efficiency.~~

Based on laboratory pump flow measurements (Komhyr et al., 1986, 1995; Johnson et al., 2002), Smit and the panel of ASOPOS (2014) and Smit et al. (2021) provided useful tables listing of pump flow correction factors and of pump flow efficiencies as a function of air pressure. These values are averaged from the experiments at the time of the ECC-ozonesonde development and the values recommended by the manufacturer. Causes of pump flow reduction (dead volume in the pump piston of the pump, pump leakage, hydraulic head pressure of the reaction solution in the reaction cell, etc.) can might vary considerably among between individual ozonesondes. In order to eliminate such observational uncertainty factors, it is necessary to accurately determine measure the pump efficiency of individual each ozonesonde in the preflight preparation. However, However, such determination is not normal practice in ozonesonde launches, as it is considered technically difficult and time-consuming. As a result, most ozonesonde profiles are produced using average pump efficiency curves.

Individual pump efficiencies have already been measured by other investigators research themes in the past. For example, the National Oceanic and Atmospheric Administration/Climate Monitoring and Diagnostics Laboratory (NOAA / CMDL) developed a bubble silicone membrane flowmeter involving the use of using silicone oil (Johnson et al., 2002), and showed that the conventionally used standard pump efficiency correction tables (Komhyr et al., 1986, 1995) were underestimated as compared to the pump efficiency correction efficiencies of the currently manufactured the ECC-ozonesondes. Also, the University of Wyoming also has measured individual pump efficiencies using an airbag evacuation contraction type flowmeter equipped with an airbag and a gear pump with high pump efficiency (Johnson et al., 2002). However, no a pump efficiency measuring systems are is currently not commercially available, we developed such a system at the Aerological Observatory in Tatenno, Japan. After examining of various measurement methods led to the, we adopted of an airbag method approach

コメントの追加 [諸藤17]: Replaced according to Referee#3's comment

"Lines 60-61: I think it is important to make the point here that measuring the efficiency of each pump is NOT normal practice in ozonesonde launches, as it is considered difficult and time-consuming. As a result, almost all ozonesonde profiles are produced using average pump efficiency curves as described in the paragraph beginning in line 62. This is a source of uncertainty that the system described in this paper eliminates. It is a major advance and should be introduced here properly, as the scientific question that this paper addresses."

コメントの追加 [諸藤18]: Replaced according to Referee#1

コメントの追加 [諸藤19]: Replaced according to Referee#1 and #2

コメントの追加 [諸藤20]: Replaced according to Referee#3's comment

"Actually, it is the pump corrections that are underestimated, not the efficiencies."

コメントの追加 [諸藤21]: Replaced according to Referee#3's comment

"Actually, it is the pump corrections that are underestimated, not the efficiencies."

コメントの追加 [諸藤22]: Replaced according to Referee#1

コメントの追加 [諸藤23]: Replaced according to Referee#2

コメントの追加 [諸藤24]: Removed according to Referee#2

method for ease of its easiness to control. ~~The system was automated in order to obtain pump efficiency measurements with uniform quality. The system was designed to perform the entire series of measurement automatically, in order to be able to obtain pump efficiency with uniform quality, and has been.~~ Since 2009, we have installed this system at Tateno, Sapporo, Naha and Syowa stations in sequence since 2009. ~~At these stations, the pump efficiency of 'each' individual ozonesonde has been measured.~~ is operationally measured at these stations, which have produced a significant body of data since installation. Because of the operational ozonesonde measurement program in the last decade, we could build up a long time series of pump efficiency measurements at those sites.

In this paper, ~~firstly in section 2, we introduce the outlines of the automated pump efficiency measuring system.~~ ~~In section 3 details; the measurement method and procedures for the using this airbag type system, Section 4 describes are explained. The calculation of pump efficiency calculation, and is described in section 4. Lastly in Section 5 covers, the statistical results for of pump efficiency~~ ies as obtained ~~from through the~~ operational observation for the current this decade and the long-term stability estimates of the pump measurement system ~~are shown.~~

2 System Overview of the system

The automated pump efficiency measuring system is roughly divided into three parts: a "Control unit", a "Pressure control unit" and a "Flow measurement unit". Figure 3 ~~outlines shows the conceptual diagram of~~ the system, and Figure 4 shows its actual appearance. The control unit is designed ~~for to~~ control of the whole ~~measurement~~ system via a PC with a module that communicates directly with peripheral equipment. The pressure control unit consists of a vacuum pump, a vacuum controller, and a digital barometer. The flow measurement unit consists of an air-bag type flowmeter in a vacuum desiccator that allows various pressure conditions down to 3 hPa.

コメントの追加 [諸藤25]: Replaced according to Referee#2

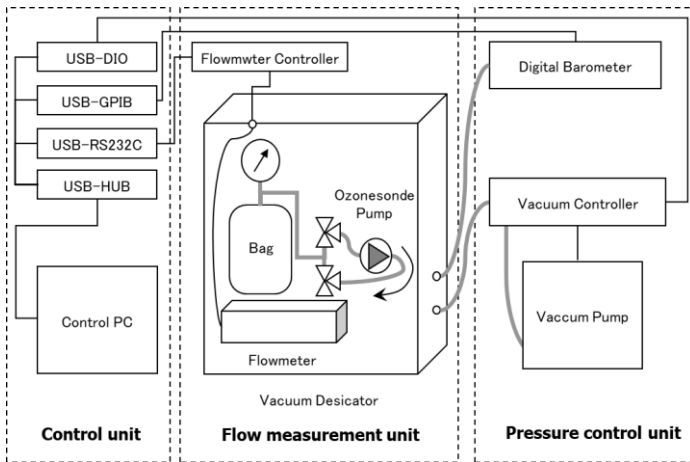


Figure 3: ~~Schematics of the automated measurement system of the pump efficiency measurement system for the electrochemical concentration cell (ECC) ozonesondes.~~



110 Figure 4: ~~Actual appearance. Picture of automated measurement system of the pump efficiency for the ECC ozonesonde.~~

The control unit consists of a Windows PC combined with various communication modules (DIO, GPIB, and RS232C) to control the entire system and collect measurement data. As these modules and the control PC are connected via USB, the system can be controlled ~~using~~by a general-purpose PC.

115 ~~The WindowsA program to control the system was developed as software running on Windows, and is used to adjust and just control~~ the pressure control unit and the flow measurement unit. ~~The program also enables has the function to~~

conversion of various measurement data acquired from the flow measurement unit at regular intervals into physical values and to collection of the data together with other information such as the digital barometer readings.

The pressure control unit controls the air pressure in the vacuum desiccator to reproduce a low-pressure environment.

As during a balloon ascent, the ozonesondes are not only subjected to decreasing atmospheric pressure, but also to and lower-temperature conditions (as low as -60 to -80°C) during balloon ascent. For this reason, we initially tried initial efforts were made to reproduce not only the low-pressure environment, but also the low-temperature environment both conditions.

However, our pump efficiency measurements for a low-temperature environment showed that temperature does not exhibit a linear relationship with pump efficiency, and even shows a negligible effect, at least in the temperature range of actual atmospheric conditions. For this reason, we decided to perform pump efficiency measurements by reproducing only with the low-pressure environmental conditions. Since the minimum pressure exhaust limit of the unit is less than 3 hPa, the entire pressure range of ozonesonde measurements can be reproduced.

By manipulating the opening degree of the exhaust valve opening in the vacuum controller with the control program, the pumping speed of the vacuum pump, (equating to the rate of i.e., the decompression speed in the desiccator), can be adjusted.

The pressurization ratespeed can also be controlled by opening and closing the solenoid valve for atmospheric pressure release.

With these adjustment functions, the air pressure in the desiccator can be maintained to within approximately ± 0.1 hPa of the target air pressure by setting the decompression ratespeed to zero during the flow measurement performed at each specified air pressure. At the start of depressurization and pressurization, a series of procedures is followed required to prevent avoid sudden air pressure changes in the desiccator, which might cause a backflow of oil from the vacuum pump to the desiccator.

The control program allows safe has the function to execution the sem steps safely.

The flow measurement unit consists of a vacuum desiccator, a flowmeter controller, and a control PC. Figure 5 shows the schematic diagram of the flow measurement unit.

コメントの追加【諸藤26】: Replaced according to Referee#2

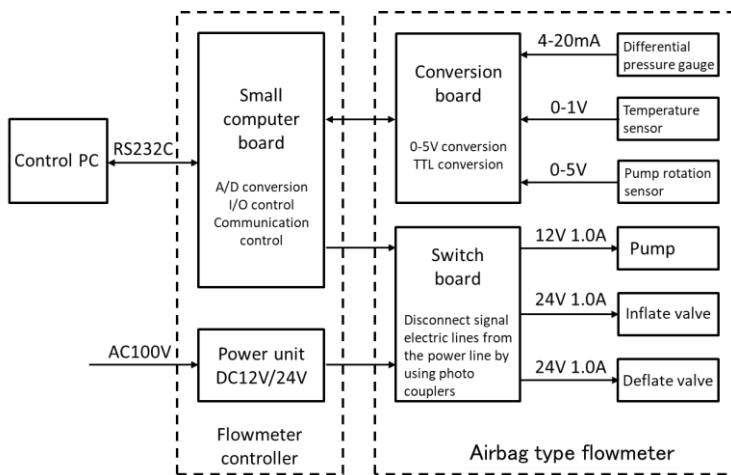


Figure 5: Schematic diagram of the flow measurement unit.

~~Inside the vacuum desiccator, the ozonesonde pump and an airbag type flowmeter are inside the vacuum desiccator located.~~

140 ~~The flowmeter controller, which is set outside the vacuum desiccator, controls the flowmeter and acquires flow values of them.~~

~~The flowmeter controller supplies power to the flowmeter, allows monitorings and controls of the flowmeter status every millisecond using the built-in microcomputer (H8/3052F), and enables sends and receives issuance/receipt of control commands and transfer of measurement data to between the control PC using RS232C. This Due to the flowmeter controller taking allows real-time measurement control on a millisecond scale care of time-dense control, thereby significantly reducing the the load of the control PC load is largely reduced.~~

145 ~~the the load of the control PC load is largely reduced.~~

The airbag type flowmeter has a conversion board to adapt the output of various sensors to the input of a small computer board, and a switch board to control the power supply of the pump and solenoid valve. The power supply lines and signal lines are electrically isolated using photo couplers to reduce noise contamination of the signal lines. Figure 6 shows the piping connection diagram of the airbag type flowmeter piping connection. The inflation and deflation valves are fluororesin three-way solenoid types valves, with NO (normally open) to COM (common) communication when not powered, and NC (normally closed) to COM communication when powered. and are By switching these valves alternately, to pump air into and out of the airbag air is taken in and out by the pump.

150 ~~connection diagram of the airbag type flowmeter piping connection. The inflation and deflation valves are fluororesin three-way solenoid types valves, with NO (normally open) to COM (common) communication when not powered, and NC (normally closed) to COM communication when powered. and are By switching these valves alternately, to pump air into and out of the airbag air is taken in and out by the pump.~~

コメントの追加 [諸藤27]: Replaced according to Referee#2

コメントの追加 [諸藤28]: Replaced according to Referee#2

コメントの追加 [諸藤29]: Replaced according to Referee#2's comment
"Just a question on what is time-dense control?".

コメントの追加 [諸藤30]: Replaced according to Referee#1

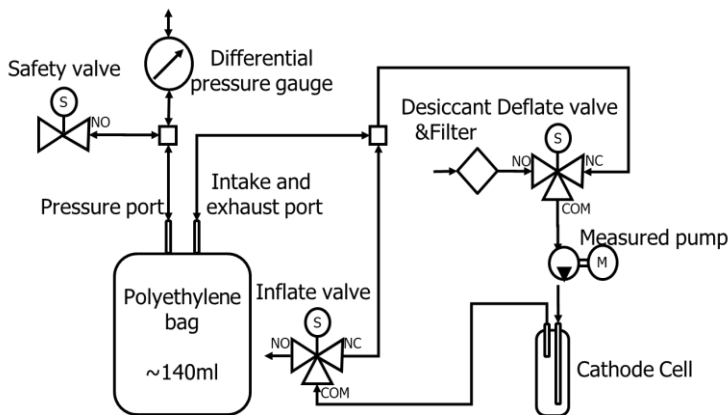


Figure 6: A Piping connection diagram of airbag type flowmeter piping connection. The 140 ml. bag is made of polyethylene. The bag is made of polyethylene in a volume of 140 ml. The inflation and deflation of the bag is conducted by using two magnet valves. The pressure between the inside and outside of the bag is measured with a differential pressure gauge. Temperatures in the bag and pump are measured by thermometers. The revolving speed of the pump is measured by an optical instrument.

The airbag is equipped with a port for differential pressure measurement separately from the intake and exhaust ports to ensure stable differential pressure measurement. A model 265 Setra Systems pressure transducer, Model-265, is used as the micro differential pressure gauge with. It has a measurement range of ± 1 hPa and an accuracy of ± 1 %FS.

The material of the airbag material must be able to deform with very weak forces, be airtight, and have little stretch/elongation and shrinkage, and should be easy to work with and/or manipulate. Among the available materials, polyethylene film with a thickness of 0.01 mm demonstrated showed the best optimal behaviour. Since in addition, wrinkles caused by uneven deformation as the airbag repeatedly in the airbag as it repeatedly expands and contracts can cause erroneous measurements, so a smaller fluoroplastic film is placed inside the bag to prevent these. After as a result of repeated prototyping, the airbag with eventually took on a shape similar to that of an intravenous drip bag was adopted.

The main control and measurement features/items of the flow measurement unit are as follows:-

- Pump ON / OFF control
- Control of flow path switching via valve by inflation/-(deflation)-valve
- Measurement of differential pressure - difference between inside/ -and- outside- of the airbag (differential pressure) - (0.01hPa) -
- Measurement of pump, temperature, temperature in the desiccator and, temperature in the airbag temperature (internal thermistor placed in it) (0.1°C)

コメントの追加 [諸藤31]: Replaced according to Referee#2

コメントの追加 [諸藤32]: Replaced according to Referee#2

コメントの追加 [諸藤33]: Replaced according to Referee#2

コメントの追加 [諸藤34]: Replaced according to Referee#3's comment
"Lines 139-140: Why does the airbag get wrinkles?"

- Measurement of pump motor speed with a handmade digital tachometer attached to the ozone sensor (0.1 rpm). (The tachometer shines light on the rotating part of the pump and detects the reflected light to determine the number of revolutions. The rotating part is partially covered with a non-reflective black sticker to. When light hits the sticker, the light is not reflected indicate, so the tachometer can measure a full revolution.)

- Time interval measurement triggered by the specified differential pressure (1msec)

3 Method for measuring pump efficiency using the airbag method

3.1 Concept Basic idea

The concept basic idea of estimating the pump flow rate (pumping power) using an airbag involves timing the inflation time from the least to the most inflated state, and the deflation time from the most inflated to the most deflated vice versa. Assuming the airbag internal volume of V_{airbag} when the most inflated/deflated states are assumed to be constant regardless of ambient pressure, as long as internal/external pressure are equal to be constant regardless of ambient pressure, the pump flow rate $S(p)$ at a given pressure p can be estimated with the averaged inflation and deflation time $t(p)$ as

$$S(p) = V_{airbag}/t(p). \quad (1)$$

The pump efficiency $k(p)$ at the given pressure p , which is defined as the ratio of the pump flow rate to that estimated at the ground-level pressure p_0 , can be calculated as follows:

$$k(p) = S(p)/S(p_0) = (V_{airbag}/t(p))/(V_{airbag}/t(p_0)) = t(p_0)/t(p). \quad (2)$$

As this equation shows, we do not need to know the exact volume of the airbag does not need to be known.

Meanwhile, on the other hand, it is necessary we have to assess whether or not the airbag is fully inflated or deflated, which is done by evaluating its internal/external in some way. Therefore, we use the differential pressure between the airbag's inside and outside. We set the threshold was set to +/- 0.8 hPa (+: inflation; -: deflation) during inflation and during deflation; we will come back to this choice as discussed later in this paper. The flow will be switched using by two valves shown in Fig. 6 when the differential pressure reached the thresholds. Figure 7 shows temporal variations in the differential pressure with elapsed time, starting from the time of the maximum deflation. A series of measurements was made when the flow will be switched at the ground-level pressure. Plotting of differential pressure during deflation from around the time of maximum inflation (red line) shows that the inflation and deflation times are equal, since they match at the time of maximum deflation. In addition, since the pump flow rate at ground level was stable, the elapsed time can be considered associated with the internal volume of the airbag. These results indicate that differential pressure values during inflation and deflation each represent a certain airbag volume. From the above, pump efficiency can be determined from equation (2) by measuring the time interval at which a certain differential pressure is observed. Since the pump flow rate at the ground level is stable, we can

コメントの追加 [諸藤35]: Replaced according to Referee#3's comment
 "I think you mean that the volume of the airbag when inflated is assumed to be the same regardless of ambient pressure, as long as the pressure inside is equal to that outside."

コメントの追加 [諸藤36]: Replaced according Referee#3's comment
 "Lines 170-177: I find this description quite confusing. I see that there is some hysteresis, but it appears that the whole point of folding the inflation and deflation curves back on each other is to show that the inflation and deflation times are equal. Could this not be simply stated?"

consider the elapsed time to be equivalent to the internal volume of the airbag. During inflation and deflation, there seems to be a hysteresis effect (blue line) in which the relationship between the differential pressure and the content volume does not match, but when it is plotted folded around the time of maximum deflation (red line), it matches. This indicates that the inflation time and deflation time are equal, and the pump repeatedly takes in and exhausts a constant volume. We have performed multiple measurements on this and have confirmed that the folded and plotted differential pressure diagrams are always the same. From the above, thus, we conclude that the differential pressure during inflation and deflation each represent a certain airbag volume, and can determine the pump efficiency from equation (2) by measuring the time interval at which a certain differential pressure (hereinafter referred to as the differential pressure threshold) is detected.

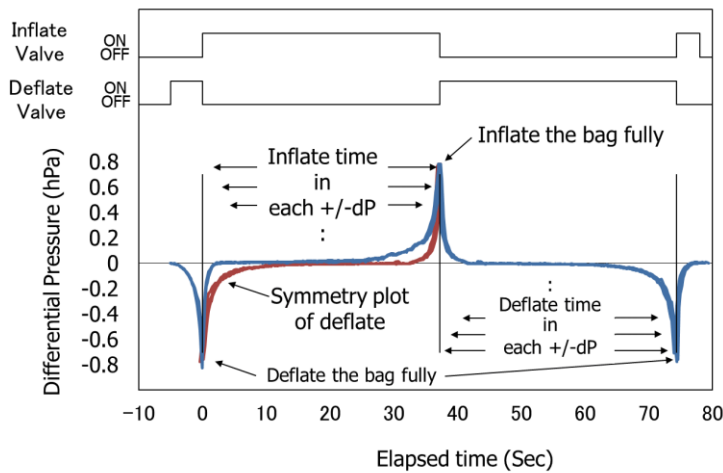


Figure 7: Schematics of pressure differences between the inside and outside of the bag as a function of lapsed time. The blue line represents plots of four-time average difference pressure values with the bag inflation/deflation of the bag is changed when the magnitude of difference pressure reaches 0.8 hPa. The red line shows a symmetric reference line of deflation to the maximum inflation at an elapsed time of approx. around 36 seconds. Also, on/off lines for of inflation and deflation are plotted at the top in the upper part of the panel.

The pump correction factor (the reciprocal of the pump efficiency) is obtained only from the time required for airbag inflation and deflation, and in the case of differential pressure Δp is expressed from equation (2) as follows. Here, the pump correction factor, which is generally the reciprocal of the pump efficiency, is used in the ECC ozonesonde observation. The factor obtained only from the time required for airbag inflation and deflation in the case of differential pressure Δp is expressed from equation (2) as follows,

$$pcf_0(p, \Delta p) = \frac{1}{k(p)} = \frac{t(p, \Delta p)}{t(p_0, \Delta p)}, \quad (3)$$

コメントの追加【諸藤37】: Replaced according to Referee#3's comment
 "This is confusing, and the first sentence seems like it belongs somewhere else in the paper. I suggest writing simply: "The pump correction factor (the reciprocal of the pump efficiency) is obtained only from the time required for airbag inflation and deflation, and in the case of differential pressure Δp is expressed from equation (2) as follows".

where $pcf_0(p, \Delta p)$ is the pump correction factor for differential pressure Δp at air pressure p and $t(p, \Delta p)$ is the time taken required to reach differential pressure Δp at air pressure p (p_0 is the ground-level pressure). In practice, however, the effects of differences in differential pressure thresholds and temperature changes due to the heat generated by solenoid valves and pump motors can cause measurement errors, giving rise to a need for consideration of a correction method.

230 The details are described in section 4.

3.2 Measurement sequence and measured value

In the series of measurements, the automated pump efficiency measuring system recorded values at pressure levels: the ground-level pressure (six times) and at 500, 200, 100, 50, 30, 20, 10, 7, 5, 4, and 3 hPa (four times each). Measurements from inflation to deflation are performed 6 times at the ground level pressure and 4 times at other pressures. In each case, as the first record was at time is the "break-in" of the airbag at each atmospheric pressure, so the values from after the second time onward were taken are used as the actual measurements measured values. The final pump correction factor finally calculated is was factor was the average value of those values observed at the time of inflation and deflation. For each measurement, the system also acquires additional data on as the time taken required for bag's internal/external the differential pressure inside and outside the airbag to reach $\pm 0.1, 0.2, 0.3, 0.4, 0.5, 0.6, 0.7, 0.8$ hPa (+:inflation; -: deflation+ during inflation, -during deflation), pump temperature, and bag internal temperature in the bag. After the cycle of measurements at the different pressure levels, six measurements at ground pressure were made are taken again to check the confirm reproducibility of the pump operation. The measurement pressure, the number of measurements, the differential pressure threshold, and other settings for this sequence of measurements can be changed in the control program.

3.3 Consideration Investigation of the back-pressure (load) effect

245 The ECC-ozonesonde has a Teflon rod protruding from the bottom of the reaction cathode cell allowing in order to guide the air intake tube from the pump to be guided appropriately properly into the reaction solution, by sliding in the tubing over the Teflon rod, which. The Teflon rod could narrow the air flow and produces give pressure resistance. Additionally, in actual ozonesonde observations, the reaction cells are filled with a solutions. As Under these situations, the back-pressure necessarily must affects the pump efficiency with these conditions. Therefore, at the first step, we investigated the back-pressure effect of the guiding Teflon rod and the reaction solution on the pump efficiency was examined. In all measurement tests, we used the same ECC-type (EN-SCI IZ) sensor was used. This section describes the outcomes results of the survey. Figure 8 (a) shows the results of a comparison between the cases in which where the pump is directly connected to the flowmeter from its the exhaust port of the pump and in which the case where the air flows goes through an empty reaction cell. This experiment showed that the pump efficiency decreased (up to approx about -6% to the maximum at 3 hPa) with by connection through the cell, and that the cell itself generated back-pressure, possibly. This back-pressure generation may be due to the presence of the Teflon rod thin line.

255

コメントの追加【諸藤38】: Replaced according to Referee#2's comment.

コメントの追加【諸藤39】: Fixed because we got the name wrong.

コメントの追加【諸藤40】: Replaced according to Referee#3's comment
""the thin line". Do you mean "the narrow tubing"?"

~~T~~Next, we examined the relationship between the volume of the reaction solution and back-pressure ~~was also examined~~. However, if ~~the~~ pump efficiency is measured with ~~an in-cell~~ the solution ~~in the cells~~, the airbag-type flowmeter will fail due to backflow caused by boiling of the solution during flow ~~observation, measurement~~ especially under low-pressure conditions.

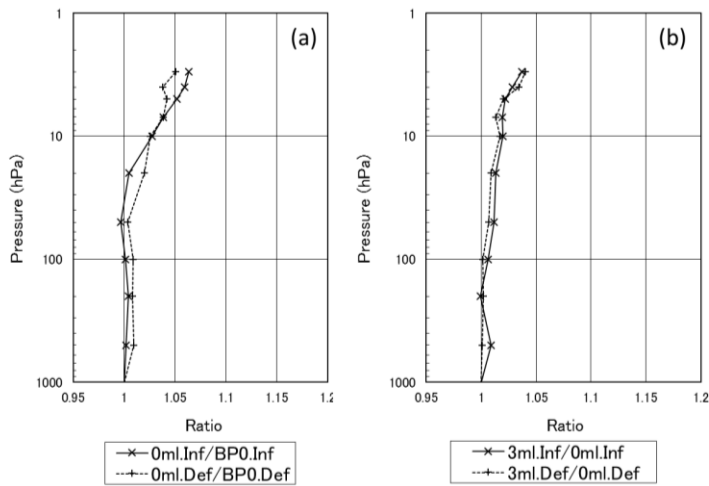
260 ~~A~~ccordingly ~~So, we used~~ silicon oil with almost the same specific density as the reaction solution ~~was used~~ instead.

Figure 8 (b) shows the results of ~~a~~ comparison between an empty reaction cell and ~~one with 3 ml of~~ an ECC-type standard reaction solution ~~volume of 3 ml. From this result, we found~~ indicate that the load ~~caused by~~ due to the reaction solution also reduced ~~the~~ pump efficiency (up to ~~approx. about~~ -4% ~~to the maximum~~ at 3 hPa). ~~T~~We considered that ~~the~~ the solution's head pressure ~~of the reaction solution causes~~ is considered to have produced this effect.

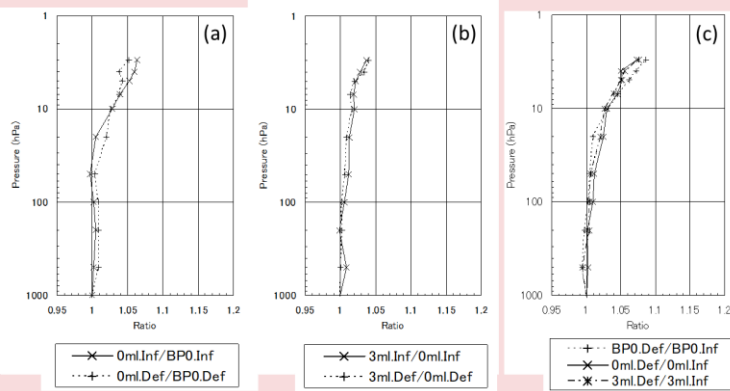
265 ~~Figure 8 (c) shows the results of a comparison of pump efficiencies during inflation and deflation under the same load conditions. Normally, the intake speed and exhaust speed of the pump are the same, and the pump efficiency should be the same at the time of intake and exhaust, but the pump efficiency during deflation is always lower than that during inflation (about 8% to the maximum at 3hPa). Since the pump efficiency shows a change tendency depending on the ambient air pressure like the change due to other loads, we consider that an additional load, presumably the dead space of the pump (as explained in section 1), is responsible for it.~~

270

コメントの追加【諸藤41】: Removed according to Referee#3's comment
"Lines 220-223: I'm not sure that these remarks, or Figure 8c, add anything to the paper. Figure 8c is not mentioned further. The remarks are also confusing, coming in the middle of a discussion about "real-world" back pressures. I suggest dropping these lines, and Figure 8c."



コメントの追加 [諸藤42]: Replaced according to Referee#3's comment
 "Lines 220-223: I'm not sure that these remarks, or Figure 8c, add anything to the paper. Figure 8c is not mentioned further. The remarks are also confusing, coming in the middle of a discussion about "real-world" back pressures. I suggest dropping these lines, and Figure 8c."



コメントの追加 [諸藤43]: Larger charactersize in legends according to Referee#1's comment
 "Larger charactersize in legends".

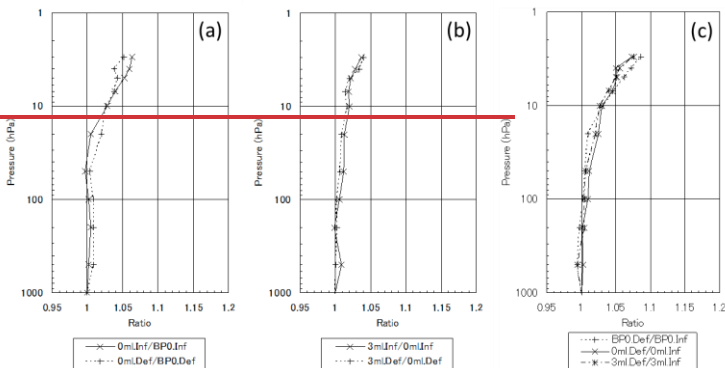


Figure 8: (a) Ratio of pump efficiency with direct when connection directly to the flowmeter from the pump exhaust port and through an empty reaction cell. (b) Ratio of pump efficiency between the case of an empty reaction cell and one with the standard the case of adding 3 ml of ECC silicon oil reaction solution, which is the standard amount of ECC type reaction solution. (c) Ratio of pump efficiency during inflation and deflation under the same load conditions. Inf: inflation; Def: deflation; BP0: back-pressure 0hPa; 0ml: no rReaction solution; 0 ml, 3ml: 3 ml of rReaction solution 3 ml.

From the abovediscussion in the previous paragraph, we conclude outcomes indicate that a filled reaction cathode cell generates a back-pressure, thereby affecting the pump efficiency, as in real atmospheric conditions. The results in Fig.9 Figure 9 reveals investigation results revealingshow the correlation of the back-pressure versus and pressure and solution volume in the cell at the ground-level pressure. BA According to this, the back-pressure is approx. about 3 hPa for the standard ECC-type reaction solution volume of 3 ml. To reproduce this load, the length and diameter of the piping were adjusted, and a load of 3 hPa was successfully applied to the exhaust side without noadding any reaction solution into the cell. All further pump correction factors reported in chapters 4 and 5 are always measured and determined with a 3 ml reaction solution in the cathode cell.

コメントの追加 [諸藤44]: Replaced according to Referee#2

コメントの追加 [諸藤45]: Removed according to Referee#3's comment

"Lines 220-223: I'm not sure that these remarks, or Figure 8c, add anything to the paper. Figure 8c is not mentioned further. The remarks are also confusing, coming in the middle of a discussion about "real-world" back pressures. I suggest dropping these lines, and Figure 8c."

コメントの追加 [諸藤46]: Added according to Referee#1's comment

"To be clear to the reader that after section 3-3 all further pump efficiencies reported in chapters 4 and 5 are always measured and determined with a 3 ml sensing solution in the cathode cell."

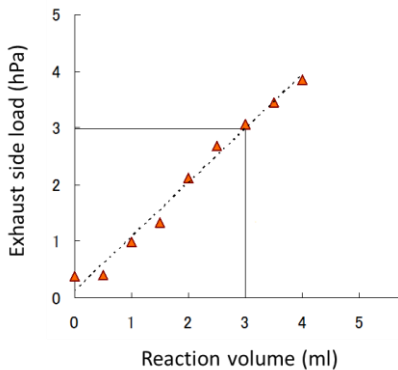


Figure 9: Exhaust side load ~~with when using~~ a reaction cell. 3 ml of ~~the~~ standard reaction solution is equivalent to a load of ~~approx. about~~ 3 hPa.

4 ~~P~~Method of calculating the pump correction factor ~~calculation~~

As ~~discussed mentioned above in the previous section, a number of there are some~~ factors ~~that~~ can cause ~~various~~ observation errors in pump efficiency measurements. ~~In this section outlines, we explain correction for such the correction method to remove these~~ errors.

4.1 Correction for ~~the effects of in-pump~~ heat generation ~~in the pump~~

The ~~study's~~ series of pump efficiency measurements ~~began with starts from the ground-level~~ pressure and continues with lower pressures ~~values~~. As the pump motor gradually ~~heat~~s up due to friction, the ~~exhaled~~ air ~~exhaled (pushed/sucked out) from the pump becomes~~ warmer in the later stages ~~of the measurement~~. ~~The volume changes~~ caused by the heating of the inflowing air ~~caused is a source of errors requiring correction in the measurement results, and should therefore be corrected for. As~~ Since the heat capacity of the air discharged from the pump is ~~relatively~~ sufficiently small, ~~it was~~ we assumed that the air ~~was~~ warmed to the same temperature as the pump ~~temperature~~ while passing through ~~in the pump~~, and the initial pump correction factor $pcf_0(p, \Delta p)$ ~~was~~ adjusted as ~~follows~~,

$$pcf_1(p, \Delta p) = pcf_0(p, \Delta p) \frac{T_{pump}(p_0, \Delta p = 0.8)}{T_{pump}(p, \Delta p = 0.8)} \quad (4)$$

where $T_{pump}(p, \Delta p)$ is the pump temperature (K) at differential pressure Δp ~~with~~ air pressure p (p_0 is ~~the~~ ground-level pressure). ~~Here, these are temperatures are the values at when the differential pressure of is 0.8 hPa (at the most inflated~~ state). ~~Table 1 shows the averaged pump temperature during pump efficiency measurements performed measured by JMA from~~

コメントの追加【諸藤47】: Replaced according to Referee#2.

コメントの追加【諸藤48】: Added according to Referee#2's comment
 "Please add the typical pump temperature observed during a test. For example, it would be helpful to know what the typical pump temperature at surface (beginning of test) and at the lowest pressure (3 hPa).".

2009 to 2022. Measurements started after 30 minutes of warm-up measurements, and the pump temperature typically increased by 5-6 °C as the measurement progressed.

310 Table 1: Pump temperature measurement results for Sapporo, Tateno, and Naha from 2009 to 2022.

Pressure (hPa)	Pump Temperature (°C) [JMA 2009 - 2022]
3	37.0 ± 2.2
4	36.7 ± 2.2
5	36.4 ± 2.2
7	36.1 ± 2.1
10	35.7 ± 2.1
20	35.4 ± 2.1
30	35.1 ± 2.1
50	34.6 ± 2.1
100	33.9 ± 2.1
200	33.1 ± 2.0
1000	31.1 ± 2.0

4.2 Correction for the effect of differential pressure effects

The measurement time is defined as ~~that~~ the time required for the pump to exhaust ~~all~~ the air and inflate the airbag ~~from~~ from zero volume to V_{airbag} or to deflate it ~~from V_{airbag} to zero~~ similarly, under atmospheric pressure p . However, the ~~air actually~~ pumped into the airbag is ~~actually~~ further inflated or (deflated) by the amount of in relation to the differential pressure $\pm\Delta p$ in addition to the ambient air pressure p . ~~By measuring the differential pressure, thus enables we can determination of whether the bag is full or empty and detect the bag content and internal volume of the airbag. There is a need to~~ We should consider ~~related~~ the effects of this on the measurement time by converting the air pressure change inside the airbag into a volume change. ~~Assuming no change in temperature, using the Boyle-Charles law (assuming no change in temperature), the internal volume of the airbag, V_{airbag} , changes with~~ by the ratio of the airbag differential pressure Δp , to the ambient air pressure p . ~~Accordingly, so~~ the measurement time t_m for the net measurement time $t(p)$, at the air pressure p is expressed as

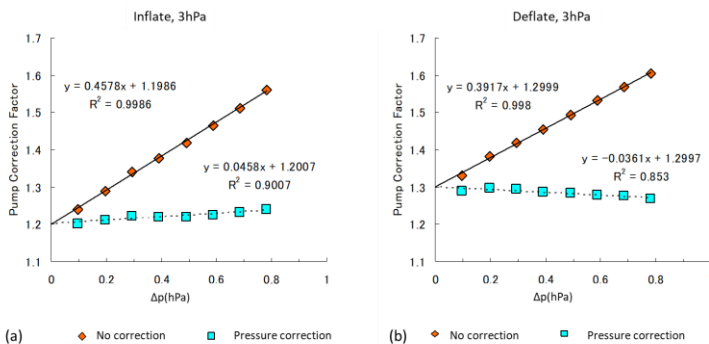
$$t_m = t(p) \cdot (1 + \Delta p/p). \quad (5)$$

コメントの追加 [諸藤49]: Added according to Referee#2's comment
"Please add the typical pump temperature observed during a test. For example, it would be helpful to know what the typical pump temperature at surface (beginning of test) and at the lowest pressure (3 hPa).".

コメントの追加 [諸藤50]: Added according to Referee#3's comment
"Lines 255-256: Why is there a differential pressure? Is that because it is the method to determine when the bag is full/empty? It might be helpful to say this.".

HereFrom this equation, itwe can be seen thatthe lower the ambient pressure p is, the values produce a larger the effect on the measurement time. To checkconfirm the effects of this operationcorrection (hereafter referred to here as the pressure correction) using t_m as the measurement time, we varied the differential pressure threshold was varied from ± 0.1 to ± 0.8 hPa in turn, obtained the pump efficiency with this correction was determined for each pressure, and comparisioned to valuesit with that without the correction was performed. Figure 10 shows the results of comparison results at an ambient pressure of 3 hPa. It can be seen that the pressure correction is generally does a good job effective, but, even after applying this correction, the correlation between the pump correction factor and the differential pressure threshold remains high. We consider the effects of the differential pressure can therefore be scenaeting as another pump loading factor on the pump. In other words Thus, if the differential pressure acts as anthe exhaust (intake) side load when the airbag is inflated (deflated), it is consistent with the results can be seen as consistent with those of the previous pressure correction. However, deriving correction for this effect is not straightforward, asbecause these loads change during measurement and eachdifferent pumps responds differently to those loads. To avoid such effects, we should make mMeasurements at even lower differential pressure thresholds should be considered to avoid such effects, but there is a limitation to the differential pressure thresholds that can be set: very lowsmall differential pressures are outside the detection limit of the micro differential pressure gauge and the measurement of time interval measurements is prone to errors. However, On the other hand, since the pump correction factor without differential pressure correction shows a very high correlation with the differential pressure threshold, we can fully use the y-intercept of the regression line can be comprehensively used as an estimate of the pump correction factor for a zero differential pressure threshold. AccordinglyTherefore, in the actual measurement, we estimate the pump correction factor corrected for the effects of the differential pressure in actual measurement can be estimated by from the regression line obtained from the measurement time taken at each of the multiple differential pressure thresholds. The pump correction factor $pcf_2(p)$ at zero differential pressure with thisobtained by the method described aboveapproach is expressed as

$$pcf_2(p) = pcf_1(p, \Delta p = 0). \quad (6)$$



345

Figure 10: Pump correction factors calculated for various different differential pressure thresholds. ValuesThe pump correction factors (representing the inverse of pump efficiency) calculated for each differential pressure threshold are plotted with and without correction and with pressure correction. The values in (a) and (b) are based on the measurement times during expansion and contraction, respectively, at 3 hPa ambient air pressure. These values were measured by connecting as determined with the pump's inlet and exhaust ports directly connected to a flowmeter.

4.3 Correction for temperature the changes in airbag capacity variations due to temperature

As the polyethylene of The airbag used for differential pressure measurement is made of polyethylene. Since polyethylene has the property of expanding and contracting with depending on the temperature, we need to consider the changes in bag the volume of the airbag during measurement must be considered. InternalThe temperature inside the airbag gradually rises during measurement because the piping leading to the airbag is heated by the heat of the solenoid valve and the circuit board inside the flowmeter housing, and the air pumped into the airbag is heated by the pump frictional heat of the pump. The temperature eventually rises by around about 5 to 10°C in a measurement sequence. Since related this variations in airbag volume is also cause a measurement error source, the pump efficiency is corrected using temperature data obtained from thermistors placed near the airbag.

After measuring the pump efficiency measurement while changing the with airbag internal temperature inside the airbag variations in a thermostatic bath, it was we found that approximate about halving of the airbag temperature change rate affected the pump correction factor. It has been confirmed that Charles' law also is obeyed held when the pump temperature was is changed using the same experimental apparatus. This is attributed likely due to the effects of the changes in airbag elongation and elasticity due to the thermal properties of the polyethylene film offsetting the effects of the volume change relating to due to Charles' law by around about half. The Based on the results of this experimental results indicated, that the pump correction factor after correction for the temperature-dependent changes in airbag capacity can be is expressed as follows:

$$pcf_3(p) = pcf_2(p) \left(1 - 0.5 \frac{T_{airbag}(p_0, \Delta p = 0.8) - T_{airbag}(p, \Delta p = 0.8)}{T_{airbag}(p_0, \Delta p = 0.8)} \right), \quad (7)$$

where $T_{airbag}(p, \Delta p)$ is the airbag temperature of the airbag (K) at differential pressure Δp with at air pressure p (p_0 is the ground-level pressure).

4.4 Application of pump efficiency measurement results to ozone partial pressure calculation

The pump efficiency $k(p)$ at atmospheric pressure p is given by the following equation (Kobayashi and Toyama, 1966b as):

$$k(p) = 1 - K \cdot \left(\frac{1}{p} - \frac{1}{p_0} \right), \quad (8)$$

where p_0 is the ground-level pressure (hPa) and K is a constant. According to Steinbrecht et al. (1998), when adiabatic change occurs in the pump, a power term (specific heat ratio $\gamma \approx 1.4$) should be is added to the second term on the right side as follows:

コメントの追加 [諸藤51]: Added according to Referee#3's comment
 "Lines 294-299: "...we found about half of the airbag temperature change rate affected the pump correction factor...". So what happened to the other half? This paragraph appears to state that "our observations only followed Charles' Law about halfway, so we used 0.5 as a fudge factor". This is not acceptable."

コメントの追加 [諸藤52]: Numbered according to Referee#3's comment
 "Line 305: This contradicts the previous equation. Which one is correct? Is the pump change adiabatic or not? By the way, all equations should be numbered."

$$k(p) = 1 - K \cdot \left(\frac{1}{p} - \frac{1}{p_0}\right)^{\frac{1}{n}} \quad (9)$$

Assuming that this is actually in reality it is a polytropic change relating to because of the effects of heat exchange with the pump in addition to the adiabatic change, the following approximate equation can be given: is given From above, the following approximate expression is given as

$$pcf(p) = \frac{1}{k(p)} = \frac{1}{1 - K \left(\frac{1}{p} - \frac{1}{p_0}\right)^{\frac{1}{n}}} = \frac{1}{1 - c_0 \left(\frac{1}{p} - \frac{1}{p_0}\right)^{\frac{1}{n}}} \quad pcf(p) = \frac{1}{1 - c_0 \left(\frac{1}{p} - \frac{1}{p_0}\right)^{\frac{1}{n}}} \quad (108)$$

where n is the polytropic index depending on the ozone sensor, c_0 is a constant depending on the ozone sensor and c_1 is $\frac{1}{n}$.

The application of the pump efficiency measurement results to the ozonesonde observations is based on $pcf_3(p)$ with the corrections described in Section 4.3. $pcf_3(p)$ is calculated from the average of three measurements in total, 3 times for each during inflation and deflation at each specified atmospheric pressure of 200 hPa or less. Using this equation, c_0 and c_1 in of the approximate equation (108) are obtained by fitting. The pump correction factor $pcf(p)$ at pressure p is then calculated from the same approximate equation (108) using the obtained constants c_0 and c_1 . Note that we do not use ground pressure data are not used because $pcf_3(p_0)$ should be 1.

5 Data from Pump efficiency data operationally obtained by the JMA's automated pump efficiency measuring system

Since 2009, JMA has comprehensively evaluated been conducting a complete inspection of EN-SCI ECC ozone sensor's pump efficiency using with the automated pump efficiency measurement system, and has been using the pump correction factors calculated from the measurement results are used to correct the ozonesonde observations from the Sapporo, Tateno, and Naha stations. This section presents the results of these measurements made over this last 13 years.

5.1 Comparison of pump correction factors between JMA and other organizations

Figure 11 shows the results of pump correction factor measurements at Sapporo, Tateno, and Naha from 2009 to 2022 using sensors with similar serial numbers had been used at each station. The values pump correction factors are were generally consistent among the stations, although the difference was with slightly larger differences at 3 hPa, where the measurement accuracy is lower.

コメントの追加【諸藤53】: Numbered according to Referee#3's comment
"Line 305: This contradicts the previous equation. Which one is correct? Is the pump change adiabatic or not? By the way, all equations should be numbered."

コメントの追加【諸藤54】: Replaced according to Referee#3's comment
"Line 305: This contradicts the previous equation. Which one is correct? Is the pump change adiabatic or not? By the way, all equations should be numbered."

コメントの追加【諸藤55】: Replaced according to Referee#3's comment
"Line 306: Please explain what approximations were used to arrive at Equation 8. The reader should be able to reproduce your analysis without guessing."

コメントの追加【諸藤56】: Fixed according to Referee#3's comment
"Line 313: $pcf_3(p_0)$ should be 1."

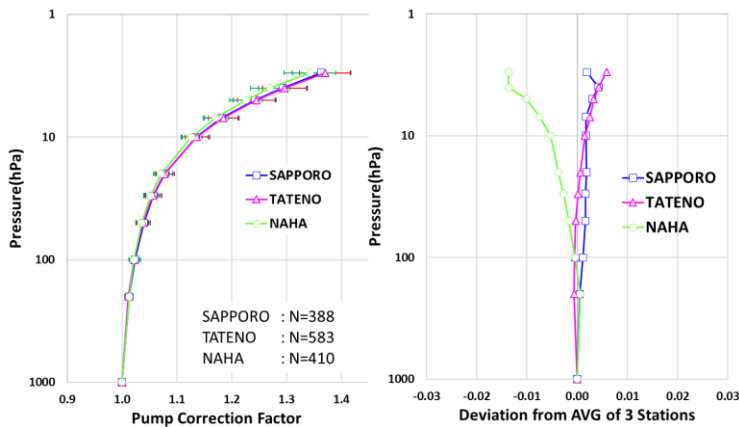


Figure 11: Pump efficiency measurement ~~for results in Sapporo and~~ Naha from 2009 to 2018, and Tateno from 2009 to 2022. The error bars in the left figure represent ~~the one-~~sigma standard deviation. ~~All The results measured at 3 sites show close correspondence are almost synchronized.~~

Figure 12 ~~shows the results~~ comparing the average pump correction factors ~~for~~ the same pump type (EN-SCI ECC) obtained by other organizations ~~with the representative measured data of with typical JMA data.~~ The pump motor specifications were ~~different~~ changed from those of the ozone sensor (serial number after post-24000 serial number -or later-) ozone sensors delivered to JMA in 2013. ~~The results indicate As a result, air pressure dependence was seen in terms of the motor speed, and suggest that speed the stability of the speed was not good was unstable depending on the among production lots. We thought that the effect was This is considered to have affecting the pump efficiency. Accordingly Therefore, assume the characteristics of current ozone sensors currently in circulation are different from those of sensors before the sensor serial number 24000, the measurement results of later sensors after the serial number 24000 are used to calculate the representative data of JMA data. As a result, air pressure dependence was seen in the motor speed, and the stability of the speed was not good. We thought that the effect was affecting the pump efficiency. Therefore, the measurement results of sensors with serial number 24000 and above are used to calculate the representative data of JMA. For the evaluation of past observation data, we show also the statistical values before the serial number pre-24000 values are shown in Table 2. The standard deviation is larger for sensors after this the serial number-24000. Stauffer et al. (2020a) also reported presents the discovery of an apparent instrument artifact that has caused a fall in total ozone measurements from around about a third of global stations to drop starting in 2014 --2016, limiting their suitability for calculating ozone trend calculation, s, and Stauffer et al. (2020b) also notes a fall drop in total column ozone in various a number of En-SCI ozonesonde sites around serial number 25250.~~

コメントの追加 [諸藤57]: Added according to Roeland Van Malderen's comment and Referee#3's comment "Line 330: Why use the measurements after #24000, rather than before #24000? You've just said that stability was not good after #24000."

コメントの追加 [諸藤58]: Added according to Roeland Van Malderen's comment.

コメントの追加 [諸藤59]: Added according to Roeland Van Malderen's comment.

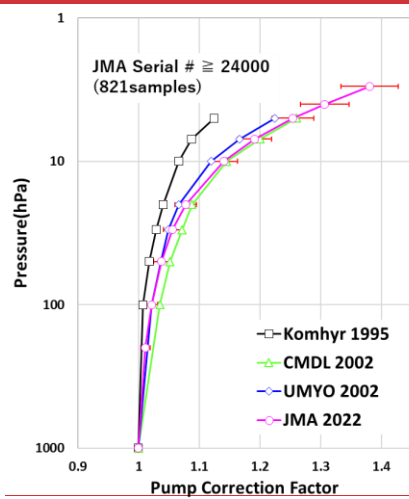
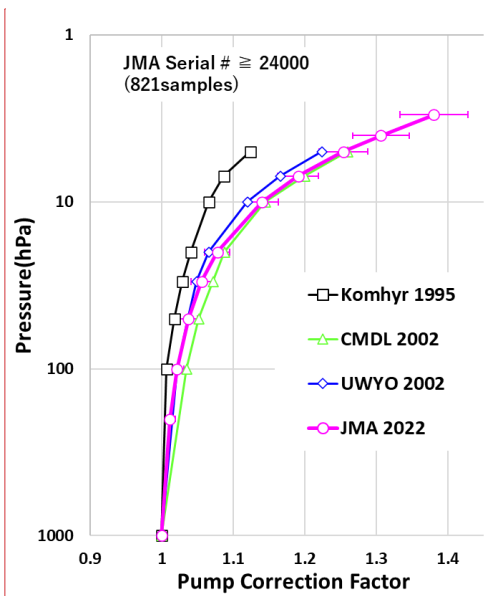
420 ~~M~~The measurements ~~were conducted by~~at the University of Wyoming ~~have been performed~~ without any ~~no~~ exhaust-side loading ~~using~~ ~~aby~~ the reaction solution, and NOAA/CMDL ~~has~~ made measurements with exhaust-side loading ~~using~~ ~~by~~ ~~non-~~ evaporative oil ~~instead of~~ ~~to~~ ~~replace~~ the ~~—~~ ~~reaction solution~~ ~~the~~ ~~reaction solution~~ (Johnson et al., 2002). We ~~replicated this work~~ ~~did that with longer~~ ~~using~~ extra tubing length ~~to create a simulated back-~~ pressure from ~~of~~ the 3ml of the reaction solution ~~with 3 ml reaction solution~~. ~~C~~According to these comparisons, ~~indicated that~~ the pump correction factors for the period during expansion ~~were~~ ~~are~~ close to ~~those~~ ~~the~~ values obtained by other organizations, and ~~that~~ the tendency in relation ~~to~~ ~~with~~ the ambient air pressure ~~was~~ ~~is~~ also similar. These ~~outcomes~~ suggest ~~the effectiveness of~~ ~~that~~ the ~~proposed~~ ~~newly developed~~ measurement system ~~is working well~~.

425 These measured pump flow efficiencies significantly differ from those ~~reported by~~ ~~published in~~ Komhyr et al. (1995). ~~This is~~ because, as noted by Smit et al. (2021), ~~pump efficiencies in~~ ~~in~~ the values of Komhyr et al. (1995) ~~in fact~~ represent ~~an~~ overall correction ~~that~~ ~~includ~~ ~~ing~~ ~~es~~ both ~~the~~ pump flow efficiency and ~~an~~ estimated ~~of~~ the stoichiometry increase over the ~~period of~~ flight.

コメントの追加【諸藤60】: Replaced according to Referee#2's comment
"Lines 335-336: It appears that "reaction solution" is being used for referring to more than one thing. It is used early in the paper when referring to the actual sensor solution (the KI salt water solution) and then in line 335 it looks like in this text "reaction solution" is referring to head pressure simulation of the sensor solution for NOAA/CMDL pump efficiency measurements, when NOAA/CMDL actually used non-evaporative oil to replace the reaction solution. Then in Line 336, I believe JMA is using extra tubing length to create a simulated back pressure of the 3cc of reaction solution.
It would be helpful to be clear where "reaction solution" is actually back pressure or simulated head pressure of the 3cc of reaction solution."

コメントの追加【諸藤61】: Replaced according to Referee#2's comment
"Lines 335-336: It appears that "reaction solution" is being used for referring to more than one thing. It is used early in the paper when referring to the actual sensor solution (the KI salt water solution) and then in line 335 it looks like in this text "reaction solution" is referring to head pressure simulation of the sensor solution for NOAA/CMDL pump efficiency measurements, when NOAA/CMDL actually used non-evaporative oil to replace the reaction solution. Then in Line 336, I believe JMA is using extra tubing length to create a simulated back pressure of the 3cc of reaction solution.
It would be helpful to be clear where "reaction solution" is actually back pressure or simulated head pressure of the 3cc of reaction solution."

コメントの追加【諸藤62】: Replaced according to Referee#2's comment
"Replace "UMYO 2002" with "UWYO 2002" within the graph for Univ of Wyoming (blue line)."
and Roeland Van Malderen's comment.



Press.	Pump Correction Factor [JMA 2022]
3	1.381 ± 0.047
4	1.307 ± 0.040
5	1.254 ± 0.034
7	1.191 ± 0.028
10	1.140 ± 0.023
20	1.078 ± 0.017
30	1.056 ± 0.015
50	1.038 ± 0.013
100	1.021 ± 0.010
200	1.011 ± 0.008

Figure 12: Comparison of pump correction factors from JMA's by our airbag method with those from other experiments. Curves of pump correction factors as a function of pressure are represented for the standard Komhyr et al. (1995) is marked by the black line with squares, and JMA pump correction factors are represented marked by the pink lined line with circles. The error bars represent the one-sigma standard deviation. Also, a curve using the NOAA/CMDL average oil bubble flowmeter values are shown is marked by the green line with triangles, and those from that using the Wyoming bag method are shown is marked by the blue line with rhombuses (Johnson et al., 2002).

Table 2: The averaged JMA pump correction factors measured by JMA for pre and the sensor serial numbers after post-24000, sensor serial numbers before 24000, and for the entire time period (2009 -2022).

Pump Correction Factor [JMA 2009 - 2022]			
Pressure (hPa)	Serial # \geq 24000 (821 samples)	Serial # < 24000 (566 samples)	ALL (1387 samples)
3	1.381 \pm 0.047	1.330 \pm 0.037	1.361 \pm 0.050
4	1.307 \pm 0.040	1.260 \pm 0.026	1.288 \pm 0.042
5	1.254 \pm 0.034	1.216 \pm 0.022	1.239 \pm 0.035
7	1.191 \pm 0.028	1.164 \pm 0.018	1.180 \pm 0.028
10	1.140 \pm 0.023	1.122 \pm 0.016	1.133 \pm 0.022
20	1.078 \pm 0.017	1.072 \pm 0.013	1.076 \pm 0.016
30	1.056 \pm 0.015	1.054 \pm 0.011	1.055 \pm 0.014
50	1.038 \pm 0.013	1.038 \pm 0.009	1.038 \pm 0.011
100	1.021 \pm 0.010	1.024 \pm 0.007	1.022 \pm 0.009
200	1.011 \pm 0.008	1.014 \pm 0.005	1.012 \pm 0.007

書式変更: 図表番号

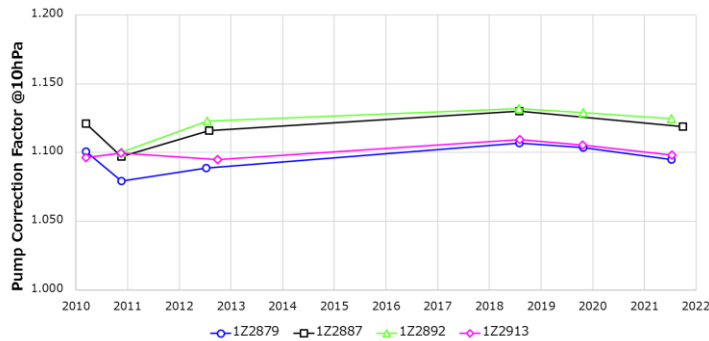
コメントの追加【諸藤63】: Added according to Roeland Van Malderen's comment.

5.2 Long-term system stability of the system

455 ~~We have investigated the long-term stability of the measurement system was examined by evaluating using results of multiple measurements on a sample data collected from of four pumps investigated at the Aerological Observatory in Tateno from 2010 to 2021. In addition to the correction outlined explained in Section 4, for this experiment only, we have corrected the pump correction factors in the experiment were according to adjusted in line with the pump motor speed as shown in the following formula in order to eliminate factor biases between the pump correction factors between the different uses of the same pump using,~~

$$460 \text{ } pcf_{corr}(p) = pcf(p) \frac{MS(p_0)}{MS(p)}, \quad (119)$$

where $pcf_{corr}(p)$ is the pump correction factor after motor speed correction at atmospheric pressure p , $pcf(p)$ is the ~~same pump correction factor before motor speed correction, at atmospheric pressure p~~ and $MS(p)$ is the motor speed at atmospheric pressure p (p_0 is the ground-level pressure). Figure 13 show ~~these multiple pump flow correction factors for the~~
465 ~~four a sample of 4 pumps exhibit. As can be seen, there is no increasing nor decreasing trends in the pump correction factors for neither of the pumps, although individual differences are seen exist. This demonstrates illustrates the long-term stability of the measurement system and freedom from the absence of any aging degradation effect.~~



470 **Figure 13: Pump correction factors at 10 hPa determined with measured by the same four sensors during the period from 2010 to 2021. Four sensors were used for the measurements.**

5.3 Decadal monitoring of an individual pump efficiency

Figure 14 shows ~~the time-series representation of individual pump correction factors at 50, 20, and 10 hPa as recorded measured at Sapporo, Tateno, and Naha stations from 2009 to 2022 (Sapporo and Naha terminated their ozonesonde observations in February 2018). At all stations, the pump correction factor exhibits temporal changes with time, showing with~~
475 a slightly increasing trend ~~along although with different slopes. The slope is larger with lower ambient pressure values to around~~

コメントの追加【諸藤64】: Added according to Referee#3's comment
"Lines 351-352: I think you mean "for this experiment only"?"

2018 - 2019 (for 50 hPa: Sapporo: +1%/9 years; Tateno: +1%/decade; Naha: +1% or less /9 years at 50 hPa; For 20 hPa: Sapporo: +2%/9 years; Tateno: +2%/decade; Naha: +2%/9 years at 20 hPa; For 10 hPa: and Sapporo: +4%/9 years; Tateno: +4%/decade; Naha: +2%/decade at 10 hPa). The serial numbers of the ozone sensors used at each station were fairly balanced. As the pump efficiency measurement system turned out to be very stable (Section 5.2), these trends of the pump correction factors should be ascribed to the ozonesonde pumps themselves.

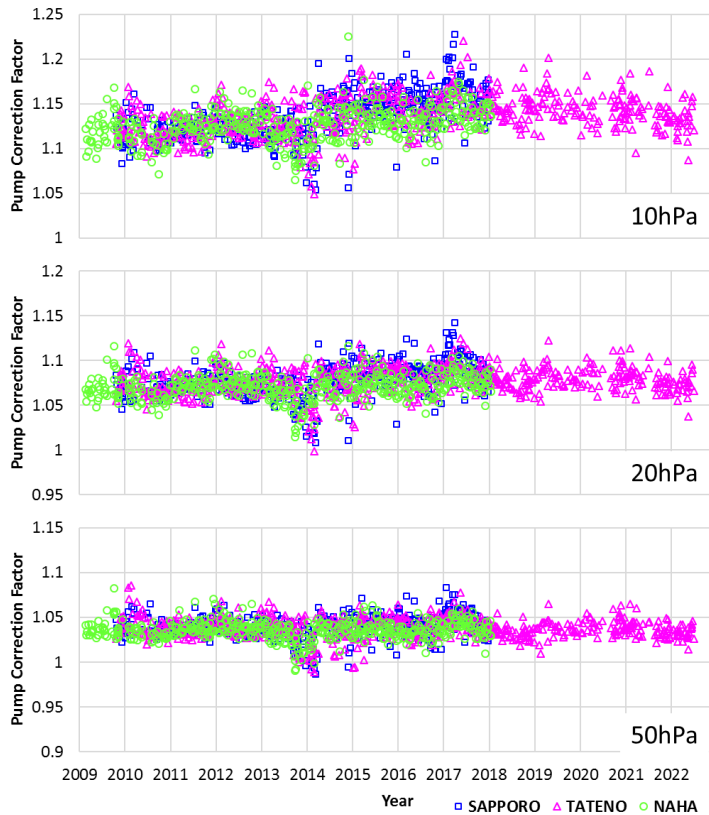
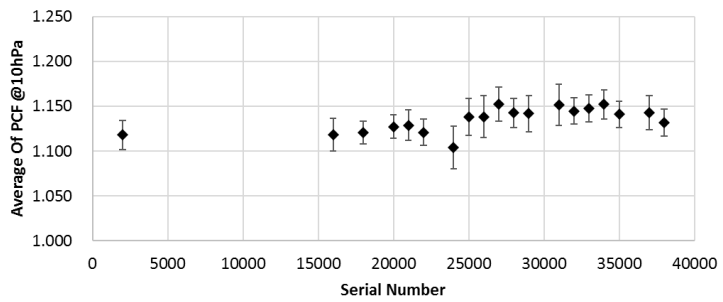
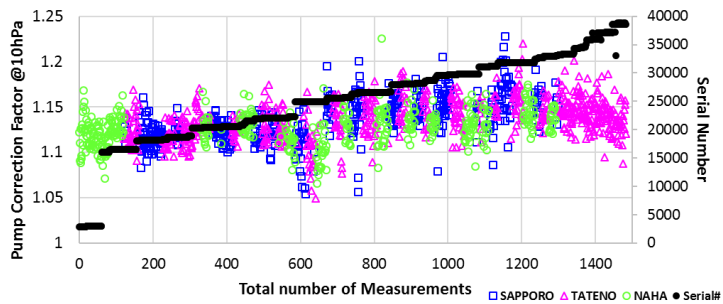


Figure 14: Pump correction factors measured for the period 2009 - 2022. (From top to bottom: 10 hPa, 20 hPa, and 50 hPa). Over this 11 years period, the pump correction coefficient factor has changed by + 1% at 50hPa, + 2% at 20hPa, and + 4% at 10hPa.

To highlight the extent to which further confirm whether this trend is caused by the pump or not, we present the pump correction factors for the different stations are presented as a function of the ozonesonde serial number in Fig. 15a. In Fig. 15b, the pump

correction factors at 10 hPa are averaged for bins of 1000 of the serial numbers. ~~It can be seen~~From these figures, we confirm that the variability of the ~~pump~~ correction factors within ~~each~~ production lot is rather modest (1.8%), and that differences between different production lots are mostly statistically insignificant.



コメントの追加 [諸藤65]: Replaced according to Referee#3's comment
 "Figure 15 (upper) appears to be wrongly labelled on the x-axis."

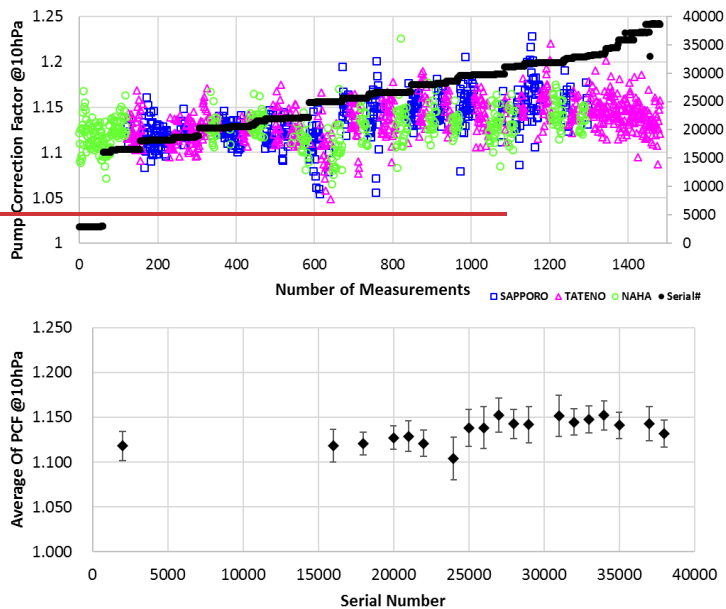
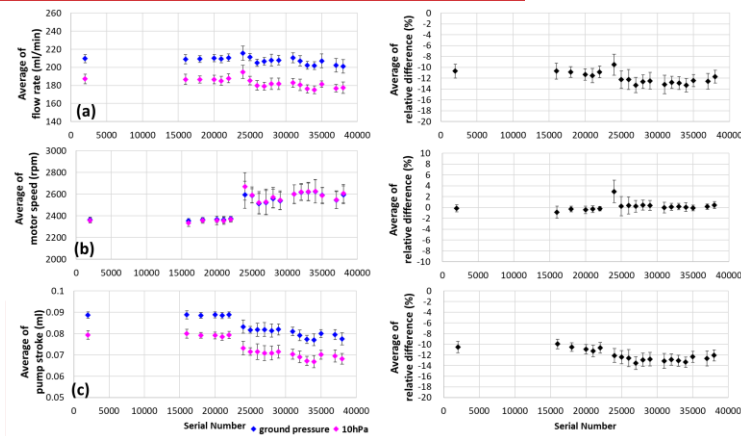
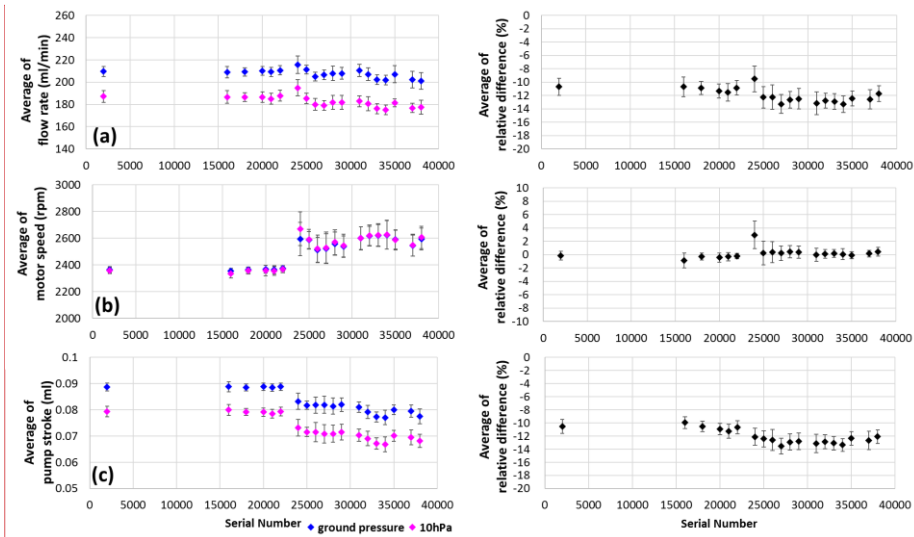


Figure 15: (Top/Upper): Pump correction factors at 10 hPa from measured during 2009 to 2022, sorted by ozone sensor serial number. Pump correction factor and ozone sensor serial number at 10hPa measured during 2009-2019. Bottom: (Lower) The same Pump correction factor at 10 hPa averaged for each bin of 1000 of ozone sensor serial numbers for measured during the period 2009 - 2022. The error bars represent in the figure below represent the one standard deviation.

Figure 16 shows a comparison of the measured values of the pump flow rate, motor speed, and pump stroke obtained by dividing the flow rate value by the motor speed value at the ground level pressure and 10 hPa. Although there is no significant change in the measured flow rate, the pump motor speed increased by about 5 to 10% and the pump stroke decreased by the same 5 to 10% after the sensor serial number 24000. This indicates we infer that a shortened pump stroke got shorter might increase the relative volumetric ratio of the pump dead space to the piston volume due to different the change of the motor specifications after the serial number 24000 (as described in Section 5.1), which may be. This might be the origin of a worse a deteriorating factor in pump efficiency. Furthermore, focusing on the deviations between the ground level pressure and 10 hPa measurements, there is little change in the motor speed differences, but with a visible trend in the pump flow rate and pump stroke differences. From this, it is we considered that the difference in pump flow rate changes between the ground and the lower pressure values; that is, the difference in measurement time changes, resulting in an increased in the pump correction factor. In all any cases, the motor characteristics fluctuate discontinuously after the serial number 24000, and the

flow rate and other characteristics of the ozone sensor change with each group of sensor serial numbers. ~~Accordingly~~~~Therefore~~, ~~we consider that~~ the increasing trend of the pump correction factor is largely ~~attributed~~~~due~~ to the sensor side.



コメントの追加【諸藤66】: Larger charactersize of axis according to Referee#1's comment
 "Larger charactersize of axis"

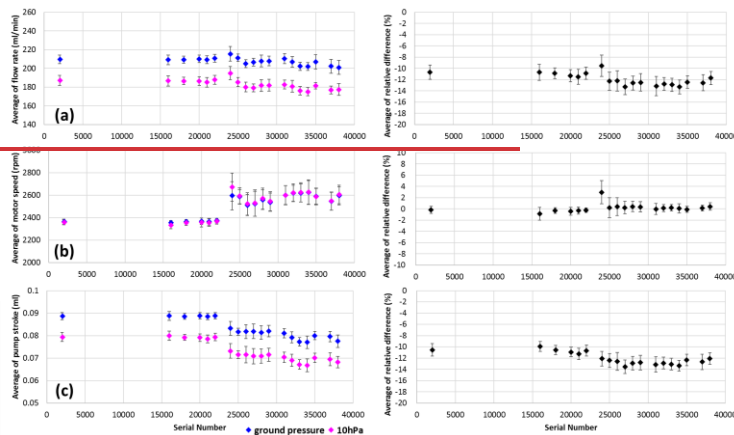


Figure 16: (a) Temporal variations in average values of pump flow rate (a), (b) pump motor speed (b), and (c) pump stroke (c) at ground pressure and 10 hPa averaged for each serial number of ozone sensors from measured during the period 2009 to 2022 (left column: measured average values; right column: relative difference to values at ground pressure).

5.4 Influence on the estimation of ozone concentration

This subsection discusses the effects of the variability caused by the changes in the characteristics of the pump flow rate outlined introduced so far on the observed data of total ozone. Fig. 17 shows the impacts on the total ozone integrated values if the table values of the pump correction factors measured by JMA for the ozone sensor serial numbers before 24000 were used instead of using the rather than measured individual pump efficiency correction values. The effects were calculated using the JMA average ozone partial pressure of JMA values for the period from 1994 to 2008; as which is a typical mid-latitude profile. The ozone partial pressure obtained using the table values for the pump efficiency correction were obtained by dividing the average partial pressure value by the measured pump correction factor and then multiplying the result that value by the table value. Each of these ozone partial pressure values at each pressure levels (the ground-level pressure, and 500, 200, 100, 50, 30, 20, 10, 7, and 5 hPa) was integrated to determine the total ozone integrated value, and the relative difference was determined for each of the pump efficiency measurements during the period from 2009 to 2022. Fig. 17 shows the relative differences of total ozone integrated values to the average that value. The total ozone integrated values are determined using the ozone partial pressure values obtained by multiplying the pump correction factor measured during the period from 2009 to 2022 for each pressure levels (the ground-level pressure, 500, 200, 100, 50, 30, 20, 10, 7, 5, 4 hPa) by the average ozone partial pressure from 1994 to 2008 corresponding to that pressure level. We confirmed that the variation in total ozone was reached about up to around 4% in the largest case. The standard deviation in the relative differences of total ozone integrated values by lot was around about 1%, and that between production lots was around about 0.6%. As per in Section 5.3, we showed that the pump correction factors tended to increase, but when a decreasing tendency

コメントの追加【諸藤67】: Replaced according to Referee#2's comment
 "The figure text letters (a) (b) and (c) should be in front of the data being described. For example: (a) Variation over time of pump flow rate."

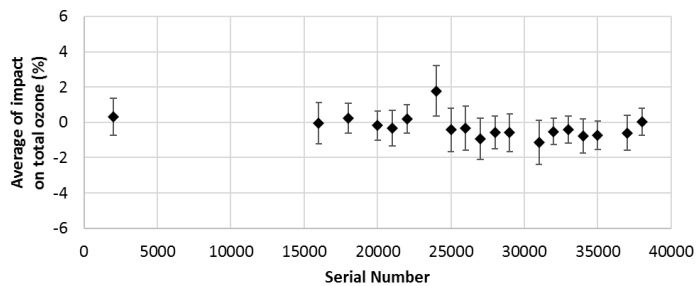
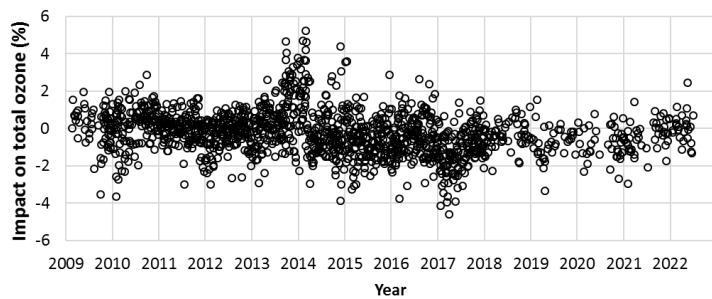
コメントの追加【諸藤68】: Replaced according to Referee#3's comment
 "Lines 403-406 (and Figure 17 caption): I am confused by this description. Should you not simply calculate the difference, for each sounding, in the total ozone found using your measured pump corrections to that using the average pump correction curve (either CMDL or your average before serial #24000 – or after serial #24000)?"

コメントの追加【諸藤69】: Added consistency with Stauffer et al. (2020a, 2020b).

was seen with converted conversion to total ozone integrated values, it tended to decrease. The fact that there is a step observed after 2014 is consistent with the drop-off of total ozone discussed pointed out by Stauffer et al. (2020a, 2020b).

535

540



コメントの追加【諸藤70】: Replaced according to Referee#3's comment
 "Lines 403-406 (and Figure 17 caption): I am confused by this description. Should you not simply calculate the difference, for each sounding, in the total ozone found using your measured pump corrections to that using the average pump correction curve (either CMDL or your average before serial #24000 – or after serial #24000)?"

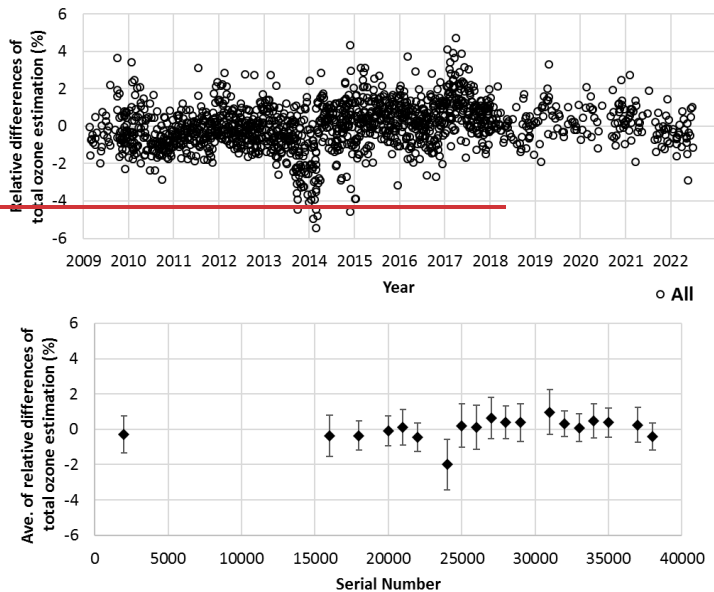


Figure 17: Top: Estimated impacts on total ozone integrated values with use of the average pump efficiency correction table. Bottom: Impacts on total ozone integrated values for each serial number lot, with error bars indicating standard deviation. (Upper) Estimation of impact on total ozone integrated values when using average pump efficiency correction table. (Lower) The impact on total ozone integrated values for each serial number lot, with the error bars indicating the standard deviation. (Upper) Relative differences of total ozone integrated values obtained from the pump correction factor measured during the period 2009-2022 and the average ozone profile (1994-2008 cumulative average). (Lower) Average of the total ozone integrated values averaged for each serial number.

6 Conclusion

The unique JMA has succeeded in developing a unique system for measuring pump efficiency, and reported here has enabled fully automatic to measure the pump efficiency measurement for of individual ECC ozonesondes fully automatically. Based on the time-series representations of the individual pump correction factors of the factors for EN-SCI ozonesondes that have been calculated by JMA using this system, we found that the factors approach indicate temporal changes over time with an increasing tendency, and also that they varied variations depending on the production lot. These effects We can be attributed this to differences in the characteristics of mechanical pumps and pump motors for each production lot. In this situation, if a table of correction values for the pump flow rate correction factor is used without individual pump efficiency measurements, the total ozone value will be affected by up to around about $\pm 4\%$.

Systematic biases ~~introduced~~ in ozonesonde observations due to ~~a change in the~~ pump performance variations can lead to erroneous stratospheric vertical ozone trend values. ~~T-In order to~~ avoid the influence of ~~the~~ lot-dependent pump correction factors in relation to EN-SCI's ozonesondes on ~~the~~ stratospheric ozone trends and to enable accurate determination of ~~deteet~~ the actual atmospheric changes with high accuracy, it is advisable we recommend to determine ~~investigate~~ the pump efficiency of each lot to pinpoint ~~understand the trend of the~~ pump correction factor trends and ~~to enable~~ adaptation ~~it~~ to the calculation of ozone concentration. ~~Although~~ ~~the production costs of this system production was not so reasonable to introduce easily~~ may at this moment ~~hinder~~ introduction at present, ~~we hope any~~ commercialization may enable the use of similar systems ~~to be commercialize at lower cost in the near future at a reasonable cost.~~

コメントの追加【諸藤71】: Replaced according to Referee#3's comment
"Line 432-433: Can such an automated system be built and operated by other stations at a reasonable cost? Can it be commercialized? If so, this recommendation would carry much more weight."

Code and Data availability

Code and data from this study are available ~~from upon request to~~ the authors upon request.

Competing interests

The ~~contact authors has~~ declared that ~~neither they nor their co-authors have any~~ an absence of competing interests.

Author contribution

TN led conceptualization and development of the automated pump efficiency measuring system. ~~ATM and TN led the~~ analyses was performed ~~presented here and prepared the paper and reported by TM and TN.~~

References

Hirota, M., and Muramatsu, H.: Performance characteristics of the ozone sensor of KC79-type ozonesonde, J. Meteorol. Res., 38, 115-118, (in Japanese), 1986.

Johnson, B. J., Oltmans, S. J., Voemel, H., Smit, H. G. J., Deshler, T., and Kroeger, C.: ECC Ozonesonde pump efficiency measurements and tests on the sensitivity to ozone of buffered and unbuffered ECC sensor cathode solutions, J. Geophys. Res., 107, D19 doi: 10.1029/2001JD000557, 2002.

Kobayashi, J., Kyojuka, M., and Muramatsu, H.: On various methods of measuring the vertical distribution of atmospheric ozone (I) – Optical-type ozone sonde, Pap. Meteor. Geophys., 17, 76–96, 1966a.

Kobayashi, J., and Toyama, Y.: On various methods of measuring the vertical distribution of atmospheric ozone (II) – Titration type chemical ozonesonde, Pap. Meteor. Geophys., 17, 97–112, 1966b.

コメントの追加【諸藤72】: Added references according to Referee#2's comment
"If available, please add a publication reference on the KI Carbon electrode type (KC) ozonesonde."

Kobayashi, J., and Toyama, Y.: On various methods of measuring the vertical distribution of atmospheric ozone (III) – Carbon iodide type chemical ozonesonde–, *Pap. Meteor. Geophys.*, 17, 113–126, 1966c.

585 Komhyr, W. D.: Electrochemical concentration cells for gas analysis, *Ann. Geophys.*, 25, 203-210, 1969.

Komhyr, W. D.: Development of an ECC-Ozonesonde, NOAA Techn. Rep., ERL 200-APCL 18ARL-149, 1971.

Komhyr, W. D.: Operations handbook - Ozone measurements to 40 km altitude with model 4A-ECC-ozone sondes, NOAA Techn. Memorandum ERL-ARL-149, 1986.

590 Komhyr, W. D., Barnes, R. A., Brothers, G. B., Lathrop, J. A., and Opperman, D. P.: Electrochemical concentration cell ozonesonde performance evaluation during STOIC 1989, *J. Geophys. Res.*, 100, 9231-9244, 1995.

Smit, H. G. J., and the Panel for ASOPOS: Quality Assurance and Quality Control for Ozonesonde Measurements in GAW, WMO GAW Rep. 201, 94pp, https://library.wmo.int/doc_num.php?explnum_id=7167, 2014.

595 Smit, H. G. J., Thompson, A. M., and the ASOPOS 2.0 Panel: Ozonesonde measurement principles and best operational practices - ASOPOS 2.0 (Assessment of Standard Operating Procedures for Ozonesondes), World Meteorological Organization GAW Rep. 268, 172pp, https://library.wmo.int/doc_num.php?explnum_id=10884, 2021.

Stauffer, R. M., Thompson, A. M., Kollonige, D. E., Witte, J. C., Tarasick, D. W., Davies, J., Vömel, H., Morris, G. A., van Malderen, R., Johnson, B. J., Querel, R. R., Selkrik, H. B., Stübi, R., and Smit, H. G. J.: A Post-2013 Dropoff in Total Ozone at a Third of Global Ozonesonde Stations: Electrochemical Concentration Cell Instrument Artifacts?, *Geophysical Research Letters*, 47, e2019GL086791. doi: 10.1029/2019GL086791, 2020a.

600 [Stauffer, R. M., Thompson, A. M., Kollonige, D. E., Tarasick, D. W., van Malderen, R., Smit, H. G. J., Vömel, H., Morris, G. A., Johnson, B. J., Cullis, P. D., Stübi, R., Davies, J., and Yan, M. M.: An Examination of the Recent Stability of Ozonesonde Global Network Data, *Earth and Space Science*, Accepted Articles, e2022EA002459. doi: 10.1029/2022EA002459, 2020b.](#)

605 Steinbrecht, W., Schwarz, R., and Claude, H.: New pump correction for the Brewer–Mast ozone sonde: Determination from experiment and instrument intercomparisons, *J. Atmos. Ocean. Tech.*, 15, 144-156, [https://doi.org/10.1175/1520-0426\(1998\)015%3C0144:NPCTB%3E2.0.CO;2](https://doi.org/10.1175/1520-0426(1998)015%3C0144:NPCTB%3E2.0.CO;2), 1998.

World Ozone and Ultraviolet Radiation Data Centre: Dataset Information: OzoneSonde, <http://dx.doi.org/10.14287/10000008>.

コメントの追加【諸藤73】: Added according to Roeland Van Malderen's comment.